Molecular Psychiatry (2020) 25:1245–1259
https://doi.org/10.1038/s41380-019-0548-4

ARTICLE

Antidepressant efficacy of a selective organic cation transporter blocker in a mouse model of depression

Alejandro Orrico-Sanchez[1] · Laetitia Chausset-Boissarie[2] · Rodolphe Alves de Sousa[2] · Basile Coutens[3] · Sara Rezai Amin[1] · Vincent Vialou[1] · Franck Louis[1] · Assia Hessani[2] · Patrick M. Dansette[2] · Teodoro Zornoza[4] · Carole Gruszczynski[1] · Bruno Giros[1,5] · Bruno P. Guiard[3] · Francine Acher[2] · Nicolas Pietrancosta[2,6] · Sophie Gautron[1]

Received: 6 December 2018 / Revised: 8 August 2019 / Accepted: 19 August 2019 / Published online: 16 October 2019

Abstract

Current antidepressants act principally by blocking monoamine reuptake by high-affinity transporters in the brain. However, these antidepressants show important shortcomings such as slow action onset and limited efficacy in nearly a third of patients with major depression disorder. Here, we report the development of a prodrug targeting organic cation transporters (OCT), atypical monoamine transporters recently implicated in the regulation of mood. Using molecular modeling, we designed a selective OCT2 blocker, which was modified to increase brain penetration. This compound, H2-cyanome, was tested in a rodent model of chronic depression induced by 7-week corticosterone exposure. In male mice, prolonged administration of H2-cyanome induced positive effects on several behaviors mimicking symptoms of depression, including anhedonia, anxiety, social withdrawal, and memory impairment. Importantly, in this validated model, H2-cyanome compared favorably with the classical antidepressant fluoxetine, with a faster action on anhedonia and better anxiolytic effects. Integrated *Z*-scoring across these depression-like variables revealed a lower depression score for mice treated with H2-cyanome than for mice treated with fluoxetine for 3 weeks. Repeated H2-cyanome administration increased ventral tegmental area dopaminergic neuron firing, which may underlie its rapid action on anhedonia. H2-cyanome, like fluoxetine, also modulated several intracellular signaling pathways previously involved in antidepressant response. Our findings provide proof-of-concept of antidepressant efficacy of an OCT blocker, and a mechanistic framework for the development of new classes of antidepressants and therapeutic alternatives for resistant depression and other psychiatric disturbances such as anxiety.

Introduction

Depression is a common and disabling disorder worldwide, with considerable clinical, social, and economic impact [1]. For over a half century, major depressive disorder has been managed primarily with medications modulating aminergic neurotransmission. This has provided the underlying

Supplementary information The online version of this article (https://doi.org/10.1038/s41380-019-0548-4) contains supplementary material, which is available to authorized users.

✉ Nicolas Pietrancosta
nicolas.pietrancosta@upmc.fr

✉ Sophie Gautron
sophie.gautron@upmc.fr

[1] Sorbonne Université, INSERM, CNRS, Neuroscience Paris Seine, 75005 Paris, France

[2] Université Paris Descartes, CNRS, 75006 Paris, France

[3] Université Paul Sabatier, CNRS, Research Center on Animal Cognition, 31062 Toulouse, France

[4] Department of Pharmacy and Pharmacy Technology and Parasitology, University of Valencia, Valencia 46010, Spain

[5] Department of Psychiatry, Douglas Mental Health Research Center, McGill University, Montreal, QC H3A 1A, Canada

[6] Present address: Sorbonne Université, École normale supérieure, PSL University, CNRS, Laboratoire des Biomolécules, 75005 Paris, France

rationale for the enduring monoamine hypothesis, which stipulates that depression results from an imbalance in serotonin (5-hydroxytryptamine, 5-HT), norepinephrine (NE), and/or dopamine (DA) signaling in the brain, which may be restored by long-term antidepressant treatment [2]. Most standard antidepressants, such as selective serotonin reuptake inhibitors (SSRIs) and norepinephrine-serotonin reuptake inhibitors (NSRIs), target high-affinity transporters for 5-HT and NE located in the plasma membrane of nerve terminals. However, these current treatments show important limitations, such as slow action onset and adverse side effects. More importantly, they do not always lead to positive outcomes, and about a third of major depression patients do not respond satisfactorily to antidepressant therapy [3]. In this context, we speculated that targeting atypical monoamine transporters such as the organic cation transporters (OCT) could constitute a relevant strategy for the discovery and development of innovative antidepressant drugs.

OCTs are facilitated diffusion transporters that participate in the absorption and clearance of various endogenous compounds and xenobiotics, by mediating their vectorial transport in renal, hepatic and placental cells [4]. These transporters can transport with low affinity (in the micromolar range) the biogenic monoamines DA, 5-HT, NE, and histamine [5–7]. Two subtypes in particular, OCT2 and OCT3, are expressed in the central nervous system [6–9], where they contribute to modulate mood-related functions, such as anxiety, response to stress, and antidepressant efficacy [9–13]. Brain OCTs have been proposed to be an alternate monoamine clearance system, prevailing in areas lacking the high-affinity transporters, or when these transporters are saturated or inhibited, for instance after antidepressant administration [9, 13, 14]. In this study, we developed a novel prodrug targeting OCT, on the assumption that it could exert antidepressant effects by engaging mechanisms differing from high-affinity transporter blockade.

Known OCT inhibitors cover a wide range of compounds, of varied efficacy and often low selectivity [4, 13]. We selected disprocynium 24 (D24), an isocyanine derivative, as lead compound for pharmacomodulation [15]. D24 is a potent and relatively selective OCT inhibitor, interacting with a putative high-affinity binding site of these transporters [16] and affinity constants ranging from 15 to 280 nM for brain OCT [17, 18]. Nevertheless, this derivative has limitations for preclinical studies or clinical use. Cyanine dyes are believed to diffuse poorly across the brain–blood barrier and have significant effects on peripheral organs [18–21]. Specifically, D24 inhibits potently α-adrenergic receptors [18], and affects OCT-mediated catecholamine clearance in sympathetically innervated tissues [19, 21]. We addressed these issues by combining molecular modeling and a prodrug delivery approach, to generate a compound with increased selectivity for OCT2. This prodrug was evaluated for its antidepressant efficacy after prolonged administration in a validated model of chronic depression, in comparison with the classical antidepressant fluoxetine. The robust behavioral effects of the prodrug, and its action on ventral tegmental area (VTA) dopaminergic neuron firing and intracellular signaling pathways demonstrate a high therapeutic potential for treatment of depressive disorders.

Material and methods

Homology modeling and drug design

Three-dimensional (3D) OCT and adrenoceptor models were built from sequence alignments and crystallographic atomic coordinates of XylE (PDB code 4GBY) and a combination of β1 adrenoceptor (PDB codes 3ZPR and 3D4S) and 5-HT1B receptor (PDB code 4IAR) using MODELER 9.0 (Discovery Studio 2016, BIOVIA, Dassault Systèmes, Vélizy-Villacoublay, France). The models were minimized and docking calculations for D24 and cyanome (Fig. 1a) were performed using CDOCKER [22]. The poses showing the lowest energy were retained and clustered according to their binding mode. 3D snapshots of the protein–ligand complexes were generated using BIOVIA DS Visualizer. Synthesis protocols, compounds characterization and full modeling and drug design procedures are detailed in Supplementary materials and methods.

In vivo detection of H2-cyanome

Brain or plasma samples were homogenized in 33% acetonitrile. Analyses were performed on a high-performance liquid chromatography–mass spectrometry (HPLC–MS/MS) system consisting of an AmaZon SL ion trap mass spectrometer (Bruker Daltonics GmbH, Bremen, Germany) equipped with an ESI interface and an Ultimate 3000 device (Dionex, Thermo Fisher Scientific, Sunnyvale, CA), a thermostated autosampler and column compartment and a UV detector. Data were acquired and processed using Hystar and the extension QuantAnalysis (version 3.2, Bruker Daltonics GmbH). HPLC separation was performed with an A/B gradient (A: 10 mM ammonium acetate, pH 4.6, and B: CH_3CN/HCOOH [999:1, vol/vol]). The column was equilibrated with 20% B for 5 min, followed by a linear gradient to B over 10 min, and 4 min in B. The column was then equilibrated with a second linear gradient from 100 to 20% B over 1 min and an isocratic concentration of 20% B over 8 min. The analysis was performed in the reversed phase mode (ACE Excel 2 C18-Amide, 2 µm, 2.1 × 150 mm, Ref. EXL-1012-1502U, AIT, Houilles, France),

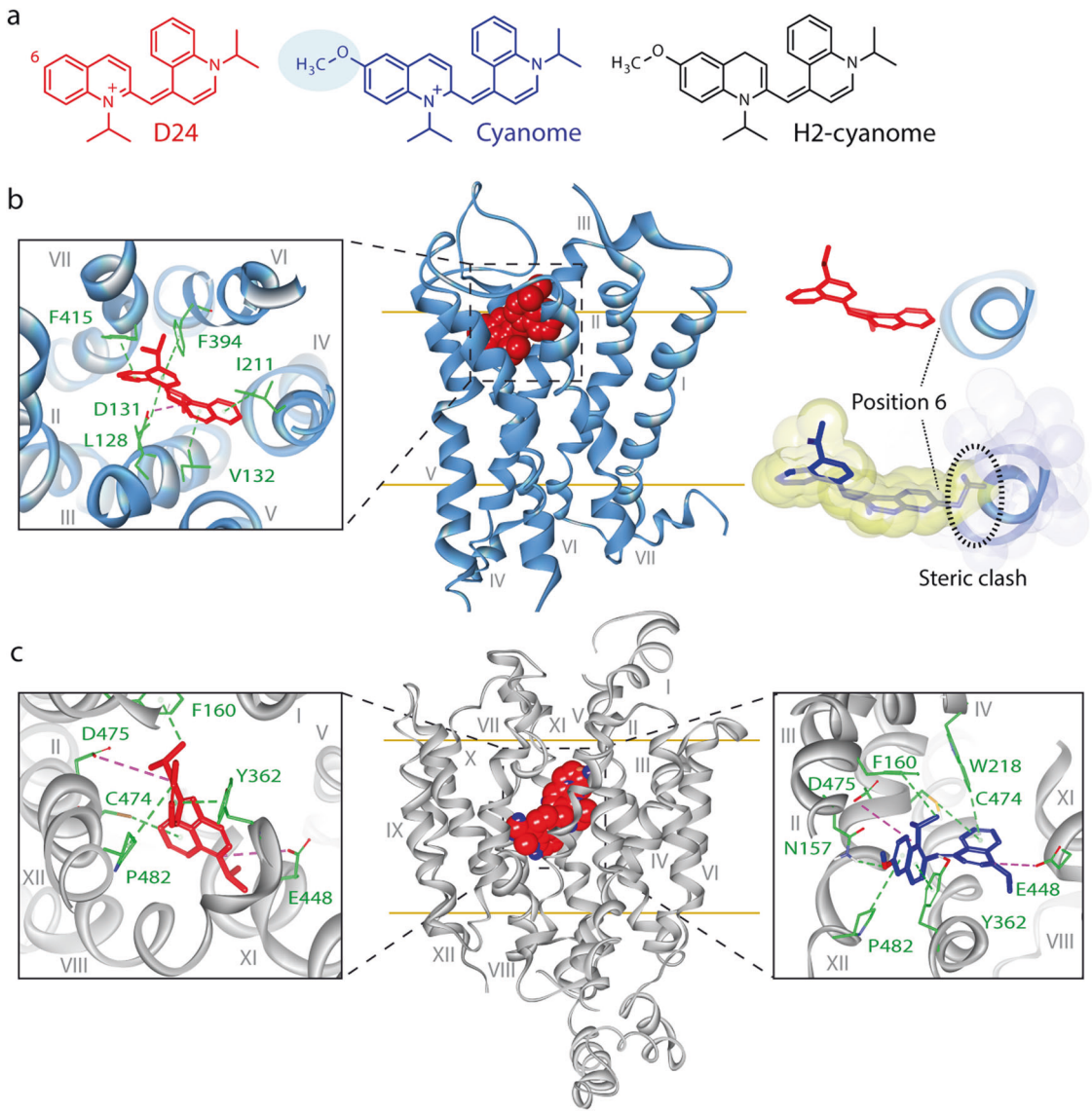

Fig. 1 Strategy for prodrug development. Design of a disprocynium (D24) analog with optimized pharmacological properties. Improvement of selectivity for OCT2 against α2-adrenergic receptor was addressed by three-dimensional homology modeling and molecular docking (**a**–**c**). Key interactions are shown in stick mode. **a** Chemical structure of D24 (red), cyanome (blue), and H2-cyanome (black). **b** Global view of D24 docked into the hα2C adrenoceptor homology model (center), characterization of chemical optimization sites on D24 (left), and selected position for steric clash introduction (right). **c** Global view of D24 and cyanome docked into the hOCT2 homology model (center) and key interactions of D24 (left) or cyanome (right). Ionic interactions are indicated by dashed red lines and hydrophobic interactions by dashed green lines. Cyanome showed a similar pattern of interaction than D24 with hOCT2, with two additional interactions, between its aromatic ring and W218, and between its 6-methoxy substituent and N157. Position 6 of D24 was substituted in cyanome with a bulky substituent hindering interaction with the fourth helix of the α2C adrenoceptor and cyanome was reduced in H2-cyanome to facilitate brain penetration

and detection was carried out in MS mode with UV wavelength scaled at 220 nm.

Behavioral studies

Animals

Male C57BL/6J mice were used for the experiments. Most behavioral studies were performed during the inactive phase (09:00–13:00) with age-matched (8–16 weeks) mice. Animals were assigned to groups without randomization. The experimenters were blinded to the treatment of the mice when performing behavioral assessments. Animal care and experiments were conducted in accordance with the European Communities Council Directive for the Care and the Use of Laboratory Animals (2010/63/UE) and approved by the French ethical committee (#5786-2016062207032685).

Model of chronic depression

To induce a chronic depression-like state, individually housed mice were administered corticosterone in drinking water (35 μg ml^{-1}; Sigma-Aldrich, Merck KGaA, Darmstadt, Germany) dissolved in 0.45% (wt/vol) hydroxypropyl-b-cyclodextrin (Sigma-Aldrich) during 10 weeks as previously reported [9, 23, 24]. Fluoxetine (15 mg/kg/day; LKT laboratories, St Paul, MN, USA) or H2-cyanome (0.1 mg/kg/day) was administered intraperitoneally (i.p.) daily during the last 3 weeks of the corticosterone regimen. Mice were tested for sucrose consumption, social interaction, open-field, elevated O-maze, and object location test, before antidepressant treatment and after 10 days and 3 weeks of treatment. The coat state was assessed weekly as a measure of motivation toward self-care. It was evaluated as the sum of the score of different parts of the body, ranging between 0 for a well-groomed coat and 1 for an unkempt coat for head, neck, dorsal/ventral coat, tail, and forepaws/hindpaws. For the sucrose preference test, singled-house mice were first habituated for 48 h to drink water from two bottles. On the following 3 days, the mice could choose between a water bottle and a 1% (wt/vol) sucrose solution bottle, with the position switched daily. Sucrose solution intake for 24 h was measured during the last 2 days and expressed as a percentage of the total amount of liquid ingested. The elevated O-maze consisted of an annular runway positioned 40 cm above the floor and divided into two opposing 90° closed sectors and two 90° open sectors. Mice were individually placed in the closed sector and their behavior recorded over a 5-min period. The time spent in each sector and the number of sector entries (a sector entry was defined as all four paws being placed in a sector) were determined by video tracking (Viewpoint, Lyon, France). The social interaction test was performed in a white open-field (42 × 42 cm) containing an empty wire mesh cage (10 × 6.5 cm) located at an extremity of the field in a low luminosity environment (25 lux). Individual mice were allowed to explore the open-field for two consecutive sessions of 2.5 min. During the second session, an unfamiliar mouse was introduced into the wire mesh cage. Between the two sessions, the test mouse was placed back into its home cage for ~1 min. The time spent by the test mouse in the interaction zone, defined as an 8-cm-wide region surrounding the mesh cage, was measured in both sessions by video tracking (Viewpoint). For the object location test, the mice were habituated during two successive days to an open-field containing an intra-field cue (one wall covered with black and white stripes). Each mouse was allowed to freely explore the open-field for a 30-min period on day 1 and for two 10-min sessions separated by 5 h on day 2. On the third day, the test mouse was allowed to explore for 5 min two identical objects (5 × 2.5 cm) positioned in two adjacent corners of the open-field (acquisition phase) then returned to its home cage for 1 h. For the sample phase trial, one of the two objects was displaced to the opposite corner of the open-field. The time spent exploring both objects was recorded over a 5-min session by video tracking. The open field consisted of a white Plexiglas field (42 × 42 cm) with the center brightly illuminated (100 lux). General locomotor activity in the center and periphery of the open field was scored for 9 min. The time and number of entries in the center zone (20 × 20 cm) were evaluated as an index of anxiety-related response. Integrated *z*-scores of depression-related variables were calculated to compare the effects of H2-cyanome with those of fluoxetine in the corticosterone depression model. Individual depression-related *z*-scores were generated with data from five tests (time and activity in the center of open-field, time and latency to enter the open zone of elevated O-maze, percentage of sucrose intake in the sucrose preference test, time of interaction in social interaction test, and coat state). Test *z* values were calculated by averaging individual *z*-scores. *Z*-score methodology was used to combine results across the different tests and the data were normalized as previously described [25]. Integrated *z*-scores were calculated after 3-week treatment with fluoxetine or H2-cyanome. For social defeat, 8-week-old C57BL/6J mice were submitted to social defeat stress for 10 consecutive days as described [26]. Only susceptible mice were treated for 3 weeks with fluoxetine (15 mg/kg/day), H2-cyanome (0.2 mg/kg/day), or saline. Social interaction tests were performed 1 day after the last day of defeat and after treatment.

Behavioral evaluation of acute treatment with H2-cyanome

For the evaluation of its acute effects in the open-field, the elevated O-maze and forced-swim tests, various doses H2-cyanome were dissolved in saline (0.9% NaCl [wt/vol]) and administered i.p. at a volume of 10 ml/kg 30 min before each test. For the forced-swim test, the mice were placed individually in a glass beaker filled with 25 ± 1 °C water to a depth of 12 cm. The duration of immobility (time during which the mice make only minimal movements to stay afloat) was recorded during the last 4 min of the 6-min testing period, after 2 min of habituation.

In vivo electrophysiological recordings of VTA DA neurons

Three types of electrophysiology experiments were performed, using either naive mice, mice administered H2-cyanome or saline for 10 days, or mice administered corticosterone during 8 1/2 weeks in combination with H2-cyanome (0.1 mg/kg/day, i.p.) or saline during the last 10 days of the corticosterone regimen. Mice were anesthetized with chloral hydrate (400 mg/kg i.p.) and placed into a stereotaxic frame. Extracellular recordings of DA neurons

in the VTA were performed using single-barreled glass micropipettes (Stoelting, Dublin, Ireland) preloaded with a 2 M NaCl solution to obtain an impedance ranging between 6–9 MΩ. Electrical signals were amplified by a high-impedance amplifier (Bak Electronics, Umatilla, OR, USA) and monitored visually with an oscilloscope (Tektronix, Beaverton, OR, USA) and audibly through an audio monitor (A.M. Systems Inc., Sequim, WA, USA). The signal was digitalized, sampled at 25 kHz and recorded on a computer using Spike2 software (Cambridge Electronic Design, Cambridge, UK). To record VTA DA neurons, the glass micropipette was positioned using the following coordinates (in mm from bregma): AP: 3.5–3.1 mm, L: ± 0.5–0.7 mm, V: −3.5 to −4.5 mm. Spontaneously active dopaminergic neurons were identified on the basis of previously established electrophysiological in vivo criteria [27]. The firing patterns of DA neurons were also analyzed to discriminate cells displaying single spikes or bursting activities. We analyzed spike-interval, and the onset of a burst was defined as the occurrence of two spikes with an inter-spike interval shorter than 0.08 s [28]. To determine the acute effects of H2-cyanome, spontaneous baseline electrophysiological activity was recorded for at least 2 min before systemic injection of H2-cyanome (0.1 mg/kg, i.p.) or cocaine (30 mg/kg, i.p.), or a combination of H2-cyanome or saline with cocaine, with a 15-min interval between the two injections. The firing rate of VTA DA neurons was then determined until neuronal activity stabilization, thereby allowing the determination of the percent of change of basal firing rate. To determine the effects of prolonged H2-cyanome treatment, spontaneous baseline activity was recorded for each neuron encountered for 2 min in mice treated with H2-cyanome or saline for 10 days. Similarly, for studies in the chronic depression model, mice were administered chronic corticosterone followed by either saline or H2-cyanome (0.1 mg/kg, i.p.) for 10 days, and electrophysiological activity was recorded successively at basal state, after an acute injection of saline, and an acute injection of H2-cyanome (0.1 mg/kg).

Western blots

Whole tissue extracts were prepared from bilateral punches (1–1.5 mm diameter; Miltex, York, PA, USA) of brain regions from adult mice at basal state, treated with corticosterone or with corticosterone plus H2-cyanome or fluoxetine. Samples were homogenized by sonication in 2 vol of ice-cold phosphate-buffered saline containing 1% Triton X-100, protease inhibitors (Complete Protease Inhibitor Cocktail, Roche Diagnostics, Meylan, France), and phosphatase inhibitors (Phosphatase Inhibitor Cocktail 3; Sigma-Aldrich). Protein concentrations were determined by Bradford's method. Protein samples (15 µg) suspended in NuPage LDS sample buffer (Invitrogen, Carlsbad, CA, USA) were separated by Bis-Tris sodium dodecyl sulfate polyacrylamide gel electrophoresis (10% gels) and transferred onto nitrocellulose membranes (Invitrogen). Transfer efficacy was controlled by Ponceau S staining. Unspecific binding sites were blocked with Tris-buffered saline containing 0.1% Tween-20 and 5% nonfat milk and membranes were immunoprobed with antibodies against glycogen synthase kinase-3β (GSK3β, 1/2000) from Millipore (Billerica, MA, USA), phosphorylated GSK3β (p GSK3β, 1/1000), Akt (1/2000), pThr308 or Ser473 Akt (1/200), phosphorylated extracellular-signal regulated kinase1/2 (pErk1/2, 1/1000) and p-P70S6 (1/500) from Cell Signaling (Danvers, MA, USA), Erk1/2 (1/1500) from Santa Cruz, or β-actin (1/2500) from Sigma-Aldrich. Membranes were incubated with infrared-labeled secondary antibodies (IRDye 700DX and IRDye 800CW; 1/5000; Rockland, Gilbertsvillle, PA, USA). Immunoblotting was quantified with an Odyssey Infrared Imaging System and Application Software version 3.0 (LI-COR Biosciences, Lincoln, NE, USA).

Statistics

PRISM (GraphPad Software, San Diego, CA, USA) was used for statistical calculations. Sample sizes for behavioral and electrophysiology experiments were chosen based on previous reports [9, 29, 30]. A posteriori sensitivity power analyses performed using G*Power 3.1 indicated that the chosen sample size allow detection of a small effect size ($f = 0.15$–0.16) for most behavioral experiments and a medium effect size ($f = 0.3$) for social defeat, a small effect size ($f = 0.09$) for electrophysiology experiments after chronic corticosterone administration, a medium to large effect size ($d = 0.57$) for electrophysiology experiments after 10-day H2-cyanome treatment, and a large effect size ($d = 0.75$–1) for electrophysiology experiments after acute treatment, with 80% power assuming a 5% significance. Sucrose preference, social interaction, elevated O-maze, coat state, open-field, forced swim, and western blot experiments were analyzed using one-way analysis of variance (ANOVA), followed by Dunnett's post-hoc test. Mann–Whitney test was used for analysis of z-scores after H2-cyanome and fluoxetine treatment. Student's t test was used for analysis of the firing of VTA neurons in untreated mice and in 10-day H2-cyanome treated mice. Object location test, social defeat, and electrophysiology data after corticosterone treatment were analyzed using two-way ANOVA, followed by Sidak post-hoc test. False discovery rate evaluation using the two-stage linear step up procedure of Benjamini, Krieger, and Yekutieli showed q-values ranging from 0.019 to < 0.0001 for behavioral experiments and coat state, and from 0.0044 to < 0.0001

for western blot analysis. Statistical significance was set at $P < 0.05$.

Results

Development of a selective OCT prodrug

To develop a new potent and selective OCT ligand, 3D homology models of the human α2-adrenergic receptor (Fig. 1b), an unwanted target, and of human OCT2 in the outward-open conformation (Fig. 1c) were generated from selected templates (Supplementary Fig. 1a–e). The OCT2 model generated was coherent with previous models [31–33], and interactions defined in functional studies [16, 34, 35]. By comparing positioning and interactions of D24 in both models, we modified this compound to introduce a bulky substituent hindering interaction with the α2C adrenoceptor, thereby generating the analog cyanome (Fig. 1a). Cyanome showed a similar docking pattern of interaction to D24 with hOCT2 (Fig. 1c). The relevance of the interactions predicted for cyanome was verified through binding and uptake experiments. Binding experiments showed that cyanome inhibited less potently the human α2C and the α2A adrenoceptors than D24 (Supplementary Fig. 1f). The observed inhibition constant (K_i) values were 185 ± 42 nM (mean ± s.e.m.) for the α2A adrenoceptor and 252 ± 32 nM for the α2C adrenoceptor (Supplementary Fig. 1f), compared with 28 and 66 nM for D24 for α2A and α2C adrenoceptors, respectively [18]. Cyanome also retained the ability to block the transport activity mediated by hOCT2 in transfected cells, with an IC_{50} value of 123 ± 26 nM (Supplementary Fig. 1f), a value comparable with that of D24 [18]. These results suggest that modification of D24 into cyanome markedly increased selectivity at hOCT2, as predicted by molecular modeling. Next, we speculated that charged cyanine analogs such as cyanome might have limited potential for use as antidepressants, due to low brain penetration. By exploiting a redox brain delivery system previously described [36], cyanome was modified into a prodrug that could more readily diffuse into the brain parenchyma and be activated therein, H2-cyanome (Fig. 1a). The fate of H2-cyanome in vivo after systemic administration was determined by HPLC and mass spectrometry analysis of mice plasma and brain extracts, at different time points after a single i.v. injection. These analyses showed that after i.p. injection H2-cyanome diffuses into the brain and is rapidly cleared from the soluble fractions of both plasma and brain (Table 1). Furthermore, to identify the potential metabolites of H2-cyanome in a physiological context, we investigated the nature of the derivatives generated after incubation with human liver microsomal preparations. Four main metabolites were identified within the first minutes of incubation, the most abundant metabolite of which was cyanome (Supplementary Fig. 2).

Table 1 Detection of H2-cyanome in plasma and brain

Time after injection (i.v.)	5 min	15 min	2 h	24 h
Plasma (ng/ml)	3.65 ± 1.69	2.15 ± 0.31	<0.5	<0.5
Brain (ng/g)	3.97 ± 2.3	0.56 ± 0.56	<0.5	ND

Data are expressed as means ± s.e.m. ($n = 6$)

i.v. intravenous, *ND* not detectable

Antidepressant effects of H2-cyanome in a chronic depression model

H2-cyanome was evaluated for its behavioral effects in male mice, in particular antidepressant efficacy. In a model of chronic depression induced by 7-week corticosterone administration [9, 23, 24], daily administration of a low dose of H2-cyanome (0.1 mg/kg, i.p.) induced rapid positive effects on several behaviors mimicking symptoms of depression, such as anhedonia, anxiety, social withdrawal, and memory impairment (Fig. 2 and Supplementary Fig. 3). The action of this compound on these parameters was as robust as those of the classical antidepressant fluoxetine (15 mg/kg). Specifically, H2-cyanome efficiently reversed the action of corticosterone on anhedonia, evaluated by sucrose preference (Fig. 2b), on social interaction (Fig. 2c), on anxiety level, evaluated by time spent in the anxiogenic zone of the elevated O-maze (Fig. 2d), by latency to enter this zone (Fig. 2e) and by time and activity in the center of the open-field (Supplementary Fig. 3b), and on short-term memory, evaluated by performance in the object location test (Fig. 2f). This last effect, similar to that exerted by fluoxetine, was confirmed in the novel object test (Supplementary Fig. 3c). Importantly, H2-cyanome showed an accelerated onset of action on anhedonia compared with fluoxetine at 11 days (Fig. 2b) and better effects on anxiety level at 21 days (Fig. 2d, e and Supplementary Fig. 3b). Finally, H2-cyanome also improved partially coat state (Fig. 2g) and induced no weight loss over time (Supplementary Fig. 3d), as fluoxetine. To evaluate more finely the effects of H2-cyanome, we applied z-normalization across measures of these depression-related variables, i.e., anxiety and anhedonia-like behaviors and coat state. Interestingly, individual *z*-scores of mice treated with H2-cyanome were significantly lower than those of mice treated with fluoxetine (Fig. 2h), suggestive of a better antidepressant effect of H2-cyanome.

Contrasting with the effects of repeated administration, acute injection of various doses of H2-cyanome had no

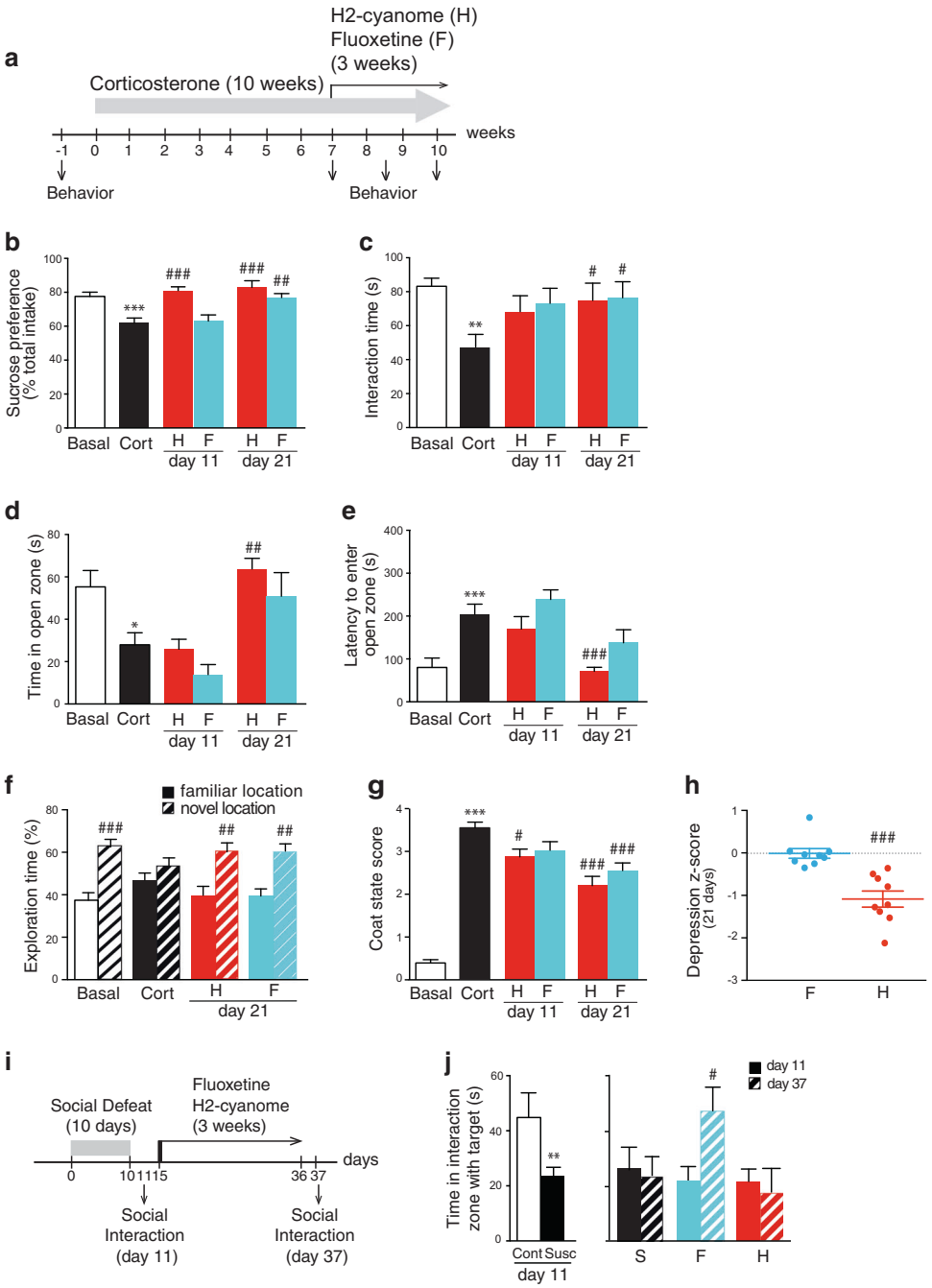

effect on locomotor activity or anxiety level in the open-field (Supplementary Fig. 4a) and elevated O-maze (Supplementary Fig. 4b). However, acute injection elicited a moderate but reproducible antidepressant-like effect on immobility in the forced-swim test, which appeared to reach a maximum at the dose of 0.1 mg/kg (Supplementary Fig. 4c). Finally, evaluation of the long-term action of H2-cyanome in another depression paradigm, social defeat, showed that this compound was not able to reverse the action of social stress on social interaction, contrarily to fluoxetine (Fig. 2i–j).

Effects of H2-cyanome systemic administration on the firing of VTA neurons

H2-cyanome was initially designed to influence monoamine neurotransmission in the brain through blockade of OCT. Based on its potent action on anhedonia in the sucrose

◀ **Fig. 2** Antidepressant efficacy of H2-cyanome in a model of chronic depression. **a** Experimental scheme for the chronic depression model induced by corticosterone. One-way analysis of variance (ANOVA) ($n = 8$–29) showed a significant effect of treatment on (**b**) sucrose preference ($F5,61 = 9.54$; $P < 0.0001$), (**c**) social interaction ($F5,57 = 2.89$; $P < 0.05$), (**d**) time ($F5,52 = 7.66$; $P < 0.0001$) and (**e**) latency ($F5,53 = 8.20$; $P < 0.001$) to enter the open zone of the elevated O-maze, and (**g**) coat state ($F5,91 = 90$; $P < 0.0001$). Dunnett's post-hoc tests indicate a significant effect of the corticosterone treatment ($^{*}P < 0.05$, $^{**}P < 0.01$, $^{***}P < 0.001$). H2-cyanome but not fluoxetine significantly increased sucrose preference (**b**) and improved coat state after 11 days (**g**). Both H2-cyanome and fluoxetine significantly increased sucrose preference (**b**) and social interaction (**c**), and improved coat state (**g**) after 21 days. H2-cyanome but not fluoxetine significantly increased the time in the open zone of the elevated O-maze (**d**) and decreased the latency to enter this zone (**e**). Dunnett's post-hoc test, $^{\#}P < 0.05$, $^{\#\#}P < 0.01$, $^{\#\#\#}P < 0.001$. For the object location test (**f**), two-way ANOVA ($n = 8$–10) showed significant main effects of object on exploration time ($F1,70 = 48.42$; $P < 0.0001$). Sidak post-hoc tests revealed significant differences before corticosterone and after H2-cyanome and fluoxetine treatment ($^{\#\#}P < 0.01$). **h** Integrated z-scores across depression-related variables in the corticosterone depression paradigm showed a lower depression score for H2-cyanome than for fluoxetine after a 3-week treatment ($n = 9$). Unpaired 2-tailed Mann–Whitney test, $^{***}P < 0.001$. Social-defeat stress (**i**) induced a profound social aversion (**j**, left panel, $n = 8$–24; Student's t test, $^{**}P = 0.01$), which was reversed by fluoxetine (17 mg/kg, i.p.) and not H2-cyanome (0.2 mg/kg, i.p.) (**j**, right panel, $n = 8$). Repeated two-way ANOVA revealed a significant time x treatment interaction ($F_{2,21} = 3.66$; $P = 0.04$). Sidak post-hoc tests revealed significant differences between day 11 and day 37 for fluoxetine-treated mice ($^{\#}P < 0.05$) but not for saline and H2-cyanome-treated mice. S saline, F fluoxetine, H H2-cyanome. Results are given as mean ± s.e.m

preference test, we speculated that H2-cyanome might have an impact on dopaminergic signaling. Dopaminergic neurons of the VTA encode reward, motivation and learning [37], functions profoundly impaired in depressed patients. We thus investigated the effects of both acute and repeated H2-cyanome administration on the firing of this neuronal population. The acute injection of H2-cyanome alone did not alter VTA dopaminergic neuron firing, but potentiated the inhibitory effect of cocaine, a DA transport blocker (Fig. 3a). Since VTA neuron firing is negatively controlled by local extracellular DA, this observation reflects an inhibitory effect of H2-cyanome on DA clearance. Remarkably, a 10-day repeated administration of H2-cyanome both in naive (Fig. 3b) and corticosterone-treated (Fig. 3c) mice exerted an opposite action, i.e., a significant increase in the firing of VTA DA neurons. In the corticosterone model, this increase in DA neuron firing was associated with an increase in the frequency of spikes in nonbursting DA neurons and in the number of spikes within burst, but not in the burst frequency (Fig. 3c). This increased activity of VTA DA neurons may have a bearing on the antidepressant efficacy of H2-cyanome in the corticosterone model. Acute injection of saline or H2-cyanome had no notable effect on any of these parameters, in mice treated mice for 10 days with saline or H2-cyanome (Fig. 3c).

Effects of H2-cyanome on intracellular signaling pathways in the brain

ERK1/2, GSK3β, and mammalian target of rapamycin (mTOR) signaling have been implicated in antidepressant response in depressed patients and in animal models [38–40]. To gain further insight into the mechanisms of action of H2-cyanome, we investigated its influence on these signaling pathways in the brain, by western blot analysis in the corticosterone depression model. We found that all three pathways (ERK1/2, GSK3β, and mTOR) were strongly modulated by chronic corticosterone treatment in mouse prefrontal cortex and hippocampus. The phosphorylation levels of ERK1/2 (Fig. 4a), Akt at Ser473 (Fig. 4c) and p70S6 (Fig. 4d) were significantly decreased in both brain areas after corticosterone, reflecting inhibition of ERK1/2, TORC2, and TORC1 pathways, respectively. Phosphorylation of GSK3β at Ser-9, a site controlling negatively its activity (Fig. 4b), was also decreased, reflecting activation of this pathway. All these alterations in activity induced by corticosterone were reversed in both brain areas after a 21-day treatment with either fluoxetine or H2-cyanome (Fig. 4a–d). Thus, H2-cyanome restored basal state ERK1/2, GSK3β, and mTOR signaling in prefrontal cortex and hippocampus as efficiently as fluoxetine in this depression model.

Discussion

There is at present a pressing need for novel well-tolerated antidepressants combining better efficacy and quicker action onset. In spite of interesting leads [41], there has been no significant paradigm shift over the last years in the pharmacological management of major depression disorder in current practice. Important shortcomings in standard treatments include poor efficacy, slow action onset, adverse side effects, and unpredictable resistance, with one-third of patients not responding adequately to two or more successive trials of treatment. We demonstrate here proof-of-concept that targeting the atypical monoamine transporter OCT is a promising strategy for the development of novel antidepressant drugs.

OCTs have been drawing increasing attention within the last decade, as evidence accumulated that they subserve major central functions, controlling anxiety, stress response, and antidepressant action [9–13]. OCT2 and OCT3 in particular have been proposed to act as a low-affinity monoamine clearance system, regulating aminergic tonus and complementing the better-known high-affinity transporters

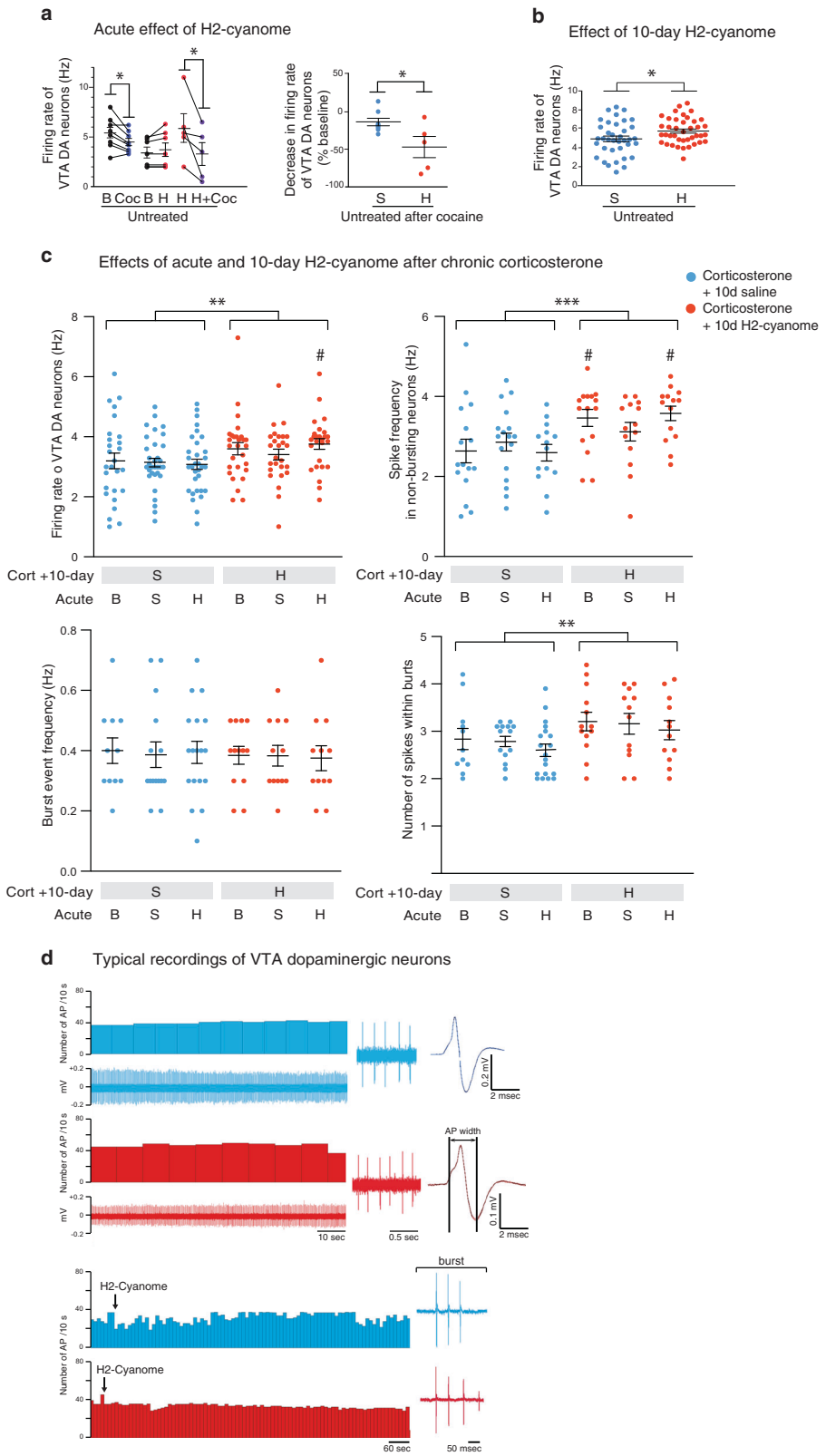

in the brain [13, 42]. However, until now, these potential therapeutic targets have been seldom exploited for drug development [32, 43]. The present study describes a novel OCT ligand with a high therapeutic potential, developed by combining molecular modeling with a prodrug brain delivery strategy.

◀ **Fig. 3** Effects of acute and chronic H2-cyanome administration on the firing of dopamine (DA) neurons of the ventral tegmental area (VTA). **a** Acute H2-cyanome administration (H) accentuated the inhibitory effect of cocaine on the firing rate of VTA DA neurons. Paired 2-tailed Student's *t* test showed significant effects of cocaine in combination or not with H2-cyanome on the firing rate of VTA DA neurons (left panel). Data represent mean ± s.e.m. firing rates. Unpaired 2-tailed Student's *t* test showed significant effects of acute H2-cyanome on percent of decrease in basal firing rate induced by cocaine (right panel). Data represent mean ± s.e.m. of decrease of percent of firing rate. **b**–**c** Ten-day H2-cyanome increased VTA DA neuron activity before and after corticosterone treatment. **b** VTA DA neuron activity after 10-day H2-cyanome treatment in untreated mice. Unpaired 2-tailed Student's *t* test, $^{*}P < 0.05$. **c** VTA DA neuron activity after 10-day H2-cyanome treatment in corticosterone-treated mice. Two-way ANOVA revealed significant main effect of 10-day H2-cyanome on firing frequency ($F_{1,65} = 7.94$; $P = 0.0054$), frequency of spikes in non-bursting DA neurons ($F_{1,84} = 13.31$; $P = 0.0005$) and number of spikes within burst ($F_{1,75} = 7.18$; $P = 0.009$), but not on burst frequency ($^{**}P < 0.01$; $^{***}P < 0.001$, 10-day H2-cyanome versus saline treatment). Sidak post-hoc tests reveal significant differences between 10-day H2-cyanome and saline in firing frequency after acute H2-cyanome, and in frequency of spikes in nonbursting DA neurons in basal state and after acute H2-cyanome ($^{\#}P < 0.05$), but no differences between basal state, acute saline, or acute H2-cyanome treatments in 10-day saline treated or H2-cyanome treated groups. Data represent means ± s.e.m. **d** Typical recordings of VTA dopaminergic neurons. Upper panel, recordings of VTA dopaminergic neurons displaying a single spike activity in mice chronically treated with corticosterone, given either in combination with saline (blue traces) or with H2-cyanone (red traces). Left, number of action potentials (APs) per 10 s recorded for 2 min. Center, isolated single APs. Right, typical example of average extracellular waveform of DA neurons. AP widths were measured from the start of the action potential to the negative trough (top) and used as a criterion to select presumed DA neurons. Lower panel, typical recordings of VTA dopaminergic neurons displaying a bursting activity in mice chronically treated with corticosterone in combination with either saline (blue traces) or H2-cyanone (red traces) and receiving an acute injection of H2-Cyanone. Left, number of APs per 10 s recorded for 15 min. Right, isolated APs showing the occurance of single spikes with a burst

In a two-step process, we generated from the OCT inhibitor D24 a ligand with increased selectivity for OCT2, which we further modified into an analog that could efficiently penetrate the brain, H2-cyanome [36]. To evaluate its antidepressant potential, we took advantage of a rodent model of chronic depression with strong construct, face and predictive validity [9, 23, 24], which surpasses acute behavioral despair tests commonly used for antidepressant screening [9, 43, 44]. In this model, prolonged corticosterone exposure induces a panel of behavioral modifications that mimic various symptoms of depression. As with human depression, these persistent depression-like anomalies can be improved by long-term, but not acute, treatment with conventional antidepressants, triggering on a longer timescale specific mechanisms [45, 46]. In this depression model, H2-cyanome compared positively to the classical antidepressant fluoxetine, with a faster action on anhedonia, evaluated by sucrose preference, and better anxiolytic

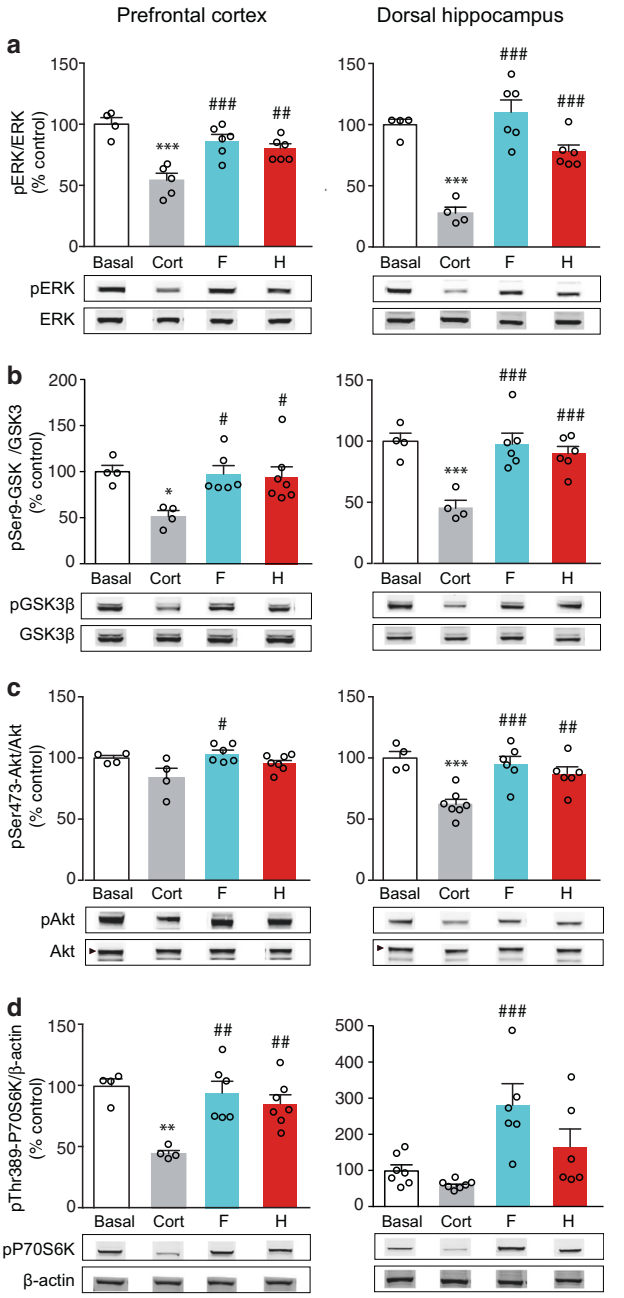

Fig. 4 Action of H2-cyanome and fluoxetine on brain intracellular signaling pathways. Chronic corticosterone administration induced alterations of activity of extracellular-signal regulated kinase1/2 (ERK1/2), glycogen synthase kinase-3β (GSK3β), and mammalian target of rapamycin (mTOR) signaling, which were reversed by either fluoxetine or H2-cyanome treatment. Quantitative western blot analysis showed alterations of phosphorylation state of ERK1/2 (**a**), pSer9 GSK3β (**b**) and pSer473 Akt (**c**), and of levels of phosphorylated p70S6 (**d**) in the prefrontal cortex (PFC) and the hippocampus (HPC). One-way analysis of variance ANOVA ($n = 4$–7) showed a significant main effect of treatment for all proteins. Dunnett post-hoc test showed significant differences between untreated and corticosterone-treated groups ($^{*}P < 0.05$, $^{**}P < 0.01$, $^{***}P < 0.001$), and significant increases after fluoxetine or H2-cyanome treatments compared with corticosterone-treated groups ($^{\#}P < 0.05$, $^{\#\#}P < 0.01$, $^{\#\#\#}P < 0.001$). Results are given as mean of phosphorylated over nonphosphorylated protein ratio ± s.e.m, or for p70S6 as mean of phosphorylated protein over β-actin ratio ± s.e.m

effects at a low dose (0.1 mg/kg; Fig. 2). Integrated *z*-scores across depression-like variables indicated a significant difference of H2-cyanome compared with fluoxetine after 3-week treatments, supporting a stronger antidepressant effect. The parameters evaluating potential toxicity were altogether encouraging (Supplementary Fig. 3 and 5, and Supplementary Table 1). Daily H2-cyanome at 0.1 mg/kg was as well tolerated as fluoxetine, with no weight loss after prolonged administration (Supplementary Fig. 3d). Blood parameters after 3 weeks of treatment were comparable with those after fluoxetine, with more favorable effects on hepatic enzymes (Supplementary Table 1). In the brain, no evident neurotoxicity was detected in various areas including dopaminergic pathways (Supplementary Fig. 5). Altogether, these results underscore the potential of H2-cyanome for depression therapy. Additional experiments are needed to refine its properties and address how it may help surmount the weaknesses of current treatments. Speed of action and durability of response to H2-cyanome should be evaluated at multiple time points during and after interruption of treatment. Information on its usefulness for resistant depression could be obtained by testing on mice selected for resistance to conventional antidepressants after social defeat or chronic mild stress (CMS).

The exact mechanisms of action of H2-cyanome in vivo remain to be clarified. A central issue is the nature of the metabolites of H2-cyanome present in the brain and their full impact on central processes, especially after prolonged exposure. OCT blockers may be suspected of acting differently than current antidepressants like SSRI and NSRI. As opposed to the high-affinity transporters gathered in aminergic terminals, OCTs are highly expressed in the cell bodies and processes (neurons and occasionally astrocytes) throughout the brain, in the principal regions receiving aminergic projections. This broad distribution and the high capacity properties of OCT, which compensate for their low-affinity, may explain their importance in the removal of extracellular monoamines [9, 13, 14]. Thus, in contrast with SSRI and NSRI, H2-cyanome by targeting OCT could regulate NE, 5-HT, and DA tone, in a widespread manner throughout the brain [13]. In addition, we cannot exclude that H2-cyanome might interact with other yet undetermined targets, exerting direct or indirect effects by competing with endogenous ligands of these targets. In particular, as the lead compound D24 shows a modest affinity for the SERT [18], potential modulation of this transporter should also be considered. Supporting an unconventional mode of action, in line with these characteristics, H2-cyanome induced few behavioral modifications when administered acutely. In particular, this compound showed only moderate antidepressant-like effects in the forced-swim test, contrarily to SSRIs and NSRIs which exert robust antiimmobility effects in behavioral despair paradigms [47].

We speculate that both limited interactions with α adrenoceptors and efficient brain penetration contribute to the robust antidepressant effects of H2-cyanome. α adrenoceptors play important roles in controlling blood pressure, heart rate, and contractility [48–50]. Based on the metabolic profile of H2-cyanome in microsomal fractions, two charged metabolites of H2-cyanome, cyanome and its demethylated derivative, are plausible candidates for mediating the antidepressant effects of the prodrug. Our experiments suggest that these two compounds should interact less potently than D24 [18] with α2A and 2C adrenoceptors in vivo, while remaining capable of blocking OCT. Central α2A adrenoceptors and α2C adrenoceptors in the adrenal medulla both exert a negative control over blood pressure and heart rate, by mediating respectively sympathoinhibition [51] and feedback control of epinephrine release [50]. Thus, restricting the antagonism at α2 adrenoceptors may be beneficial to avoid unwanted cardiovascular effects. Importantly, interactions with central α2 adrenoceptors could also play a part in the antidepressant efficacy of H2-cyanome, but it is at this stage difficult to predict to what extent α2 blockade is a disadvantage. Some previous studies suggest that restricting α2A antagonism might improve antidepressant action and anxiety [52, 53], while others suggest on the contrary that α2 adrenoceptor blockade could contribute to the pharmacological activity of antidepressants [54], or potentiate their action [55]. Finally, we also believe that choice of D24 as lead scaffold was critical for favoring interactions with central OCT and limiting potential adverse side effects. Other cyanine dyes such as decynium 22 (D22) can also inhibit OCT, with overall less affinity than D24 [4, 18, 56]. However, while both D24 and D22 inhibit peripheral α1 adrenoceptors [57], D22 has a 50-fold higher affinity for these receptors than D24 [18] or cyanome (data not shown), restricting its use in vivo due to its pronounced hypotensive action [57]. These mechanisms may also have a bearing on the adverse effects of D22 on locomotor activity [43]. Considering the diversity of functions attributed to α adrenoceptors both at periphery and in the brain, optimization of H2-cyanome in future developments may require refining selectivity. In particular, development and in-depth studies of H2-cyanome derivatives may allow to identify molecules with optimal binding properties at OCT and α adrenoceptor subtypes for clinical use.

In vivo electrophysiological recordings revealed a complex action of H2-cyanome on DA signaling in the brain, on two distinct time scales. Our experiments showed that in naive mice acute H2-cyanome could potentiate the inhibitory effects of cocaine, a DA transporter inhibitor, on the

firing of VTA neurons. DA levels in the VTA have been shown to negatively modulate VTA DA neuron firing [58], via inhibitory somatodendritic D2 receptors [59]. These results suggest that acute H2-cyanome could dampen DA neuron activity synergistically with cocaine by increasing local DA concentrations, through the inhibition of OCT-mediated DA clearance in this brain region. To gain a full understanding of the action of the prodrug, additional in vivo and ex vivo experiments are required to determine whether acute H2-cyanome affects also the clearance of NE and 5-HT, and that of DA in other brain areas.

Another notable effect of H2-cyanome, this time with a direct bearing on antidepressant response, was the effect of prolonged H2-cyanome administration. Contrarily to acute injection, a 10-day H2-cyanome treatment in naive or corticosterone-treated animals was associated with an increased firing frequency of VTA DA neurons. Previous evidence demonstrate that VTA DA neurons display multiple activity modes [60]. The fine analysis of the changes in the firing pattern in the corticosterone model revealed subtle effects of 10-day H2-cyanome treatment, including an increase in spike frequency in nonbursting neurons and in the number of spikes within burst. These modifications may underlie the antidepressant efficacy of H2-cyanome in the corticosterone model of chronic depression. VTA DA-releasing neurons display a remarkable functional heterogeneity, with distinct subpopulations controlling motivated behaviors in a complex manner [37, 61]. Their activation has been associated with reward and motivation [37], functions often altered in MDD patients. More specifically, the activity of VTA DA neurons was decreased in animals submitted to CMS, a classical depression paradigm [62, 63], and their optogenetic activation was shown to reverse the depression-like behaviors induced in this paradigm [64]. In keeping with these results, in our experiments the firing frequency of VTA DA neurons was lowered after chronic corticosterone exposure (Fig. 4b, c). Unpaired 2-tailed Student's t test showed significant decrease after chronic corticosterone treatment followed by 10-day saline injection compared with 10-day saline injection alone ($^{***}P < 0.001$). In the social defeat model, on the contrary, susceptible animals showed increased firing rate and burst firing of VTA DA neurons [65]. In line with these latter findings, optogenetic phasic activation of these neurons increased susceptibility to social-defeat stress, an effect relying mainly on NAc-projecting but not mPFC-projecting DA neurons [66]. Further supporting a differential effect of these projections, optogenetic inhibition of NAc-projecting neurons was shown to induce resilience, while inhibition of mPFC-projecting neurons increased susceptibility [66]. Such opposing roles of distinct DA neuron subpopulations in the VTA, and their differential activation depending on the type of stressor and model, could explain why H2-cyanome showed potent effects in the corticosterone-induced depression model but seemed ineffective after social defeat stress. In particular, activation of VTA DA neurons could play a key role in the efficacy of H2-cyanome on behaviors reflecting anhedonia such as sucrose preference, at an early stage when fluoxetine is still inactive (Fig. 2). The nature of the precise VTA DA neuron populations engaged in these effects of H2-cyanome has yet to be determined.

At another level, our study discloses main effects of H2-cyanome on intracellular signaling pathways involved in the regulation of mood and in antidepressant efficacy. The MAP kinase ERK1/2 was previously shown to be inhibited in prefrontal cortex and hippocampus of depressed suicide victims [67] and activated by long-term antidepressant treatment in animal models of depression [23]. Abnormal GSK3β activity has been found in prefrontal cortex of individuals with major depressive disorder [68, 69], and inhibition of GSK3β shown to play a role in antidepressant action [39]. The mTOR intracellular pathway has been proposed to underlie the fast-acting antidepressant effects of ketamine in humans [40]. In our model, all three pathways responded to corticosterone, in parallel with the emergence of depression-related behavioral anomalies. Remarkably, the beneficial effects on these behaviors of a 3-week treatment with either fluoxetine or H2-cyanome were associated with a return to basal activation states, similar to those before corticosterone treatment. Altogether, these experiments indicate that H2-cyanome modulates these intracellular regulatory pathways in a similar way than fluoxetine, suggesting at least in part common regulatory mechanisms within the brain, downstream of aminergic signaling.

In conclusion, we have devised through molecular modeling and pharmacomodulation a novel OCT-targeted drug with increased selectivity, which can penetrate the brain. Its antidepressant efficacy in a validated depression model demonstrates a high potential for therapeutic use, compared with the conventional antidepressant fluoxetine. Our findings provide a conceptual and mechanistic framework for the design of selective OCT ligands, which may open a field of discovery for new classes of antidepressants with improved properties.

Acknowledgements We thank J-P Guilloux (UMRS 1178, Université Paris-Saclay) for help with z-scoring, F. Machulka at the rodent phenotyping facility of Institut de Biologie Paris-Seine for expert assistance with animal care, and C. Betancur for critical reading of the paper. Financial support was provided by the Agence Nationale de la Recherche (ANR-13-SAMENTA-0003-01) and SATT Lutech.

Author contributions NP, FA, and SG conceived the study. NP conceived and performed molecular modeling, and designed the compounds. NP, AH, and PMD performed microsomal fraction analysis. NP, LC-B, and RAD.S synthetized the compounds. AOS, SRA, and VV performed behavioral analyses. BPG designed the

electrophysiological studies. BPG and BC performed and analyzed the electrophysiological studies. AOS performed western blot analyses. AOS and TZ participated in HPLC/MS analysis. BG provided key facilities, equipment, and advice. FL and CG performed the histochemical experiments. SG coordinated the study. NP, AOS, BPG, and SG wrote the paper. All authors reviewed and approved the paper.

Compliance with ethical standards

Conflict of interest The authors declare that they have no conflict of interest.

Publisher's note Springer Nature remains neutral with regard to jurisdictional claims in published maps and institutional affiliations.

References

1. Kessler RC, Angermeyer M, Anthony JC, DEG R, Demyttenaere K, Gasquet I, et al. Lifetime prevalence and age-of-onset distributions of mental disorders in the World Health Organization's World Mental Health Survey Initiative. World Psychiatry. 2007;6:168–76.
2. Wong ML, Licinio J. Research and treatment approaches to depression. Nat Rev Neurosci. 2001;2:343–51.
3. Rush AJ, Trivedi MH, Wisniewski SR, Nierenberg AA, Stewart JW, Warden D, et al. Acute and longer-term outcomes in depressed outpatients requiring one or several treatment steps: a STAR*D report. Am J Psychiatry. 2006;163:1905–17.
4. Koepsell H, Lips K, Volk C. Polyspecific organic cation transporters: structure, function, physiological roles, and biopharmaceutical implications. Pharm Res. 2007;24:1227–51.
5. Grundemann D, Koster S, Kiefer N, Breidert T, Engelhardt M, Spitzenberger F, et al. Transport of monoamine transmitters by the organic cation transporter type 2, OCT2. J Biol Chem. 1998;273:30915–20.
6. Wu X, Kekuda R, Huang W, Fei YJ, Leibach FH, Chen J, et al. Identity of the organic cation transporter OCT3 as the extraneuronal monoamine transporter (uptake2) and evidence for the expression of the transporter in the brain. J Biol Chem. 1998;273:32776–86.
7. Amphoux A, Vialou V, Drescher E, Bruss M, Mannoury La Cour C, Rochat C, et al. Differential pharmacological in vitro properties of organic cation transporters and regional distribution in rat brain. Neuropharmacology. 2006;50:941–52.
8. Busch AE, Karbach U, Miska D, Gorboulev V, Akhoundova A, Volk C, et al. Human neurons express the polyspecific cation transporter hOCT2, which translocates monoamine neurotransmitters, amantadine, and memantine. Mol Pharm. 1998;54:342–52.
9. Bacq A, Balasse L, Biala G, Guiard B, Gardier AM, Schinkel A, et al. Organic cation transporter 2 controls brain norepinephrine and serotonin clearance and antidepressant response. Mol Psychiatry. 2012;17:926–39.
10. Vialou V, Balasse L, Callebert J, Launay JM, Giros B, Gautron S. Altered aminergic neurotransmission in the brain of organic cation transporter 3-deficient mice. J Neurochem. 2008;106:1471–82.
11. Wultsch T, Grimberg G, Schmitt A, Painsipp E, Wetzstein H, Breitenkamp AF, et al. Decreased anxiety in mice lacking the organic cation transporter 3. J Neural Transm. 2009;116:689–97.
12. Courousse T, Bacq A, Belzung C, Guiard B, Balasse L, Louis F, et al. Brain organic cation transporter 2 controls response and vulnerability to stress and GSK3beta signaling. Mol Psychiatry. 2015;20:889–900.
13. Courousse T, Gautron S. Role of organic cation transporters (OCTs) in the brain. Pharm Ther. 2015;146:94–103.
14. Daws LC. Unfaithful neurotransmitter transporters: focus on serotonin uptake and implications for antidepressant efficacy. Pharm Ther. 2009;121:89–99.
15. Russ H, Engel W, Schomig E. Isocyanines and pseudoisocyanines as a novel class of potent noradrenaline transport inhibitors: synthesis, detection, and biological activity. J Med Chem. 1993;36:4208–13.
16. Gorbunov D, Gorboulev V, Shatskaya N, Mueller T, Bamberg E, Friedrich T, et al. High-affinity cation binding to organic cation transporter 1 induces movement of helix 11 and blocks transport after mutations in a modeled interaction domain between two helices. Mol Pharm. 2008;73:50–61.
17. Grundemann D, Schechinger B, Rappold GA, Schomig E. Molecular identification of the corticosterone-sensitive extraneuronal catecholamine transporter. Nat Neurosci. 1998;1:349–51.
18. Amphoux A, Millan MJ, Cordi A, Bonisch H, Vialou V, Mannoury la Cour C, et al. Inhibitory and facilitory actions of isocyanine derivatives at human and rat organic cation transporters 1, 2 and 3: a comparison to human alpha 1- and alpha 2-adrenoceptor subtypes. Eur J Pharm. 2010;634:1–9.
19. Russ H, Sonna J, Keppler K, Baunach S, Schomig E. Cyanine-related compounds: a novel class of potent inhibitors of extraneuronal noradrenaline transport. Naunyn Schmiedebergs Arch Pharm. 1993;348:458–65.
20. Graefe KH, Friedgen B, Wolfel R, Bossle F, Russ H, Schomig E. 1,1'-Diisopropyl-2,4'-cyanine (disprocynium24), a potent uptake2 blocker, inhibits the renal excretion of catecholamines. Naunyn Schmiedebergs Arch Pharm. 1997;356:115–25.
21. Trendelenburg U. The extraneuronal uptake and metabolism of catecholamines. In: Trendelenburg U, Weiner N, editors. Handbook of Experimental Pharmacology. 90/I. Berlin: Springer; 1988. p. 279–319.
22. Wu G, Robertson DH, Brooks CL 3rd, Vieth M. Detailed analysis of grid-based molecular docking: a case study of CDOCKER-A CHARMm-based MD docking algorithm. J Comput Chem. 2003;24:1549–62.
23. Gourley SL, Wu FJ, Kiraly DD, Ploski JE, Kedves AT, Duman RS, et al. Regionally specific regulation of ERK MAP kinase in a model of antidepressant-sensitive chronic depression. Biol Psychiatry. 2008;63:353–9.
24. David DJ, Samuels BA, Rainer Q, Wang JW, Marsteller D, Mendez I, et al. Neurogenesis-dependent and -independent effects of fluoxetine in an animal model of anxiety/depression. Neuron. 2009;62:479–93.
25. Guilloux JP, Seney M, Edgar N, Sibille E. Integrated behavioral z-scoring increases the sensitivity and reliability of behavioral phenotyping in mice: relevance to emotionality and sex. J Neurosci Methods. 2011;197:21–31.
26. Berton O, McClung CA, Dileone RJ, Krishnan V, Renthal W, Russo SJ, et al. Essential role of BDNF in the mesolimbic dopamine pathway in social defeat stress. Science. 2006;311:864–8.
27. Grace AA, Bunney BS. Intracellular and extracellular electrophysiology of nigral dopaminergic neurons—3. Evidence for electrotonic coupling. Neuroscience. 1983;10:333–48.
28. Grace AA, Bunney BS. The control of firing pattern in nigral dopamine neurons: single spike firing. J Neurosci. 1984;4:2866–76.
29. Vialou V, Robison AJ, Laplant QC, Covington HE 3rd, Dietz DM, Ohnishi YN, et al. DeltaFosB in brain reward circuits mediates resilience to stress and antidepressant responses. Nat Neurosci. 2010;13:745–52.

30. Guiard BP, El Mansari M, Blier P. Cross-talk between dopaminergic and noradrenergic systems in the rat ventral tegmental area, locus ceruleus, and dorsal hippocampus. Mol Pharm. 2008;74:1463–75.
31. Dakal TC, Kumar R, Ramotar D. Structural modeling of human organic cation transporters. Comput Biol Chem. 2017;68:153–63.
32. Pan X, Iyer KA, Liu H, Sweet DH, Dukat M. A new chemotype inhibitor for the human organic cation transporter 3 (hOCT3). Bioorg Med Chem Lett. 2017;27:4440–5.
33. Turkova A, Zdrazil B. Current advances in studying clinically relevant transporters of the solute carrier (SLC) family by connecting computational modeling and data science. Comput Struct Biotechnol J. 2019;17:390–405.
34. Popp C, Gorboulev V, Muller TD, Gorbunov D, Shatskaya N, Koepsell H. Amino acids critical for substrate affinity of rat organic cation transporter 1 line the substrate binding region in a model derived from the tertiary structure of lactose permease. Mol Pharm. 2005;67:1600–11.
35. Keller T, Gorboulev V, Mueller TD, Dotsch V, Bernhard F, Koepsell H. Rat organic cation transporter 1 contains three binding sites for substrate 1-methyl-4-phenylpyridinium per monomer. Mol Pharm. 2019;95:169–82.
36. Bodor N, Prokai L, Wu WM, Farag H, Jonalagadda S, Kawamura M, et al. A strategy for delivering peptides into the central-nervous-system by sequential metabolism. Science. 1992;257:1698–1700.
37. Morales M, Margolis EB. Ventral tegmental area: cellular heterogeneity, connectivity and behaviour. Nat Rev Neurosci. 2017;18:73–85.
38. Duman CH, Schlesinger L, Kodama M, Russell DS, Duman RS. A role for MAP kinase signaling in behavioral models of depression and antidepressant treatment. Biol Psychiatry. 2007;61:661–70.
39. Beaulieu JM, Gainetdinov RR, Caron MG. Akt/GSK3 signaling in the action of psychotropic drugs. Annu Rev Pharm Toxicol. 2009;49:327–47.
40. Li N, Lee B, Liu RJ, Banasr M, Dwyer JM, Iwata M, et al. mTOR-dependent synapse formation underlies the rapid antidepressant effects of NMDA antagonists. Science. 2010;329:959–64.
41. Harmer CJ, Duman RS, Cowen PJ. How do antidepressants work? New perspectives for refining future treatment approaches. Lancet Psychiatry. 2017;4:409–18.
42. Baganz NL, Horton RE, Calderon AS, Owens WA, Munn JL, Watts LT, et al. Organic cation transporter 3: keeping the brake on extracellular serotonin in serotonin-transporter-deficient mice. Proc Natl Acad Sci USA. 2008;105:18976–81.
43. Krause-Heuer AM, Fraser-Spears R, Dobrowolski JC, Ashford ME, Wyatt NA, Roberts MP, et al. Evaluation of the antidepressant therapeutic potential of isocyanine and pseudoisocyanine analogues of the organic cation decynium-22. Eur J Med Chem. 2017;137:476–87.
44. Horton RE, Apple DM, Owens WA, Baganz NL, Cano S, Mitchell NC, et al. Decynium-22 enhances SSRI-induced antidepressant-like effects in mice: uncovering novel targets to treat depression. J Neurosci. 2013;33:10534–43.
45. Levinstein MR, Samuels BA. Mechanisms underlying the antidepressant response and treatment resistance. Front Behav Neurosci. 2014;8:208.
46. Krishnan V, Nestler EJ. The molecular neurobiology of depression. Nature. 2008;455:894–902.
47. Cryan JF, Mombereau C, Vassout A. The tail suspension test as a model for assessing antidepressant activity: review of pharmacological and genetic studies in mice. Neurosci Biobehav Rev. 2005;29:571–625.
48. Docherty JR. Subtypes of functional alpha1-adrenoceptor. Cell Mol Life Sci. 2010;67:405–17.
49. Hein L, Altman JD, Kobilka BK. Two functionally distinct alpha2-adrenergic receptors regulate sympathetic neurotransmission. Nature. 1999;402:181–4.
50. Brede M, Philipp M, Knaus A, Muthig V, Hein L. alpha2-adrenergic receptor subtypes—novel functions uncovered in gene-targeted mouse models. Biol Cell. 2004;96:343–8.
51. Makaritsis KP, Johns C, Gavras I, Altman JD, Handy DE, Bresnahan MR, et al. Sympathoinhibitory function of the alpha(2A)-adrenergic receptor subtype. Hypertension. 1999;34:403–7.
52. Schramm NL, McDonald MP, Limbird LE. The alpha(2a)-adrenergic receptor plays a protective role in mouse behavioral models of depression and anxiety. J Neurosci. 2001;21:4875–82.
53. Wang B, Wang Y, Wu Q, Huang HP, Li S. Effects of alpha2A adrenoceptors on norepinephrine secretion from the locus coeruleus during chronic stress-induced depression. Front Neurosci. 2017;11:243.
54. Fernandez-Pastor B, Ortega JE, Grandoso L, Castro E, Ugedo L, Pazos A, et al. Chronic citalopram administration desensitizes prefrontal cortex but not somatodendritic alpha2-adrenoceptors in rat brain. Neuropharmacology. 2017;114:114–22.
55. Yanpallewar SU, Fernandes K, Marathe SV, Vadodaria KC, Jhaveri D, Rommelfanger K, et al. Alpha2-adrenoceptor blockade accelerates the neurogenic, neurotrophic, and behavioral effects of chronic antidepressant treatment. J Neurosci. 2010;30:1096–109.
56. Fraser-Spears R, Krause-Heuer AM, Basiouny M, Mayer FP, Manishimwe R, Wyatt NA, et al. Comparative analysis of novel decynium-22 analogs to inhibit transport by the low-affinity, high-capacity monoamine transporters, organic cation transporters 2 and 3, and plasma membrane monoamine transporter. Eur J Pharm. 2019;842:351–64.
57. Russ H, Friedgen B, Konigs B, Schumacher C, Graefe KH, Schomig E. Pharmacokinetic and alpha 1-adrenoceptor antagonistic properties of two cyanine-type inhibitors of extraneuronal monoamine transport. Naunyn Schmiedebergs Arch Pharm. 1996;354:268–74.
58. Einhorn LC, Johansen PA, White FJ. Electrophysiological effects of cocaine in the mesoaccumbens dopamine system: studies in the ventral tegmental area. J Neurosci. 1988;8:100–12.
59. Guiard BP, Chenu F, El Mansari M, Blier P. Characterization of the electrophysiological properties of triple reuptake inhibitors on monoaminergic neurons. Int J Neuropsychopharmacol. 2011;14:211–23.
60. Oster A, Faure P, Gutkin BS. Mechanisms for multiple activity modes of VTA dopamine neurons. Front Comput Neurosci. 2015;9:95.
61. Walsh JJ, Han MH. The heterogeneity of ventral tegmental area neurons: projection functions in a mood-related context. Neuroscience. 2014;282:101–8.
62. Chang CH, Grace AA. Amygdala-ventral pallidum pathway decreases dopamine activity after chronic mild stress in rats. Biol Psychiatry. 2014;76:223–30.
63. Moreines JL, Owrutsky ZL, Grace AA. Involvement of infralimbic prefrontal cortex but not lateral habenula in dopamine attenuation after chronic mild stress. Neuropsychopharmacology. 2017;42:904–13.
64. Tye KM, Mirzabekov JJ, Warden MR, Ferenczi EA, Tsai HC, Finkelstein J, et al. Dopamine neurons modulate neural encoding and expression of depression-related behaviour. Nature. 2013;493:537–41.
65. Cao JL, Covington HE 3rd, Friedman AK, Wilkinson MB, Walsh JJ, Cooper DC, et al. Mesolimbic dopamine neurons in the brain reward circuit mediate susceptibility to social defeat and antidepressant action. J Neurosci. 2010;30:16453–8.
66. Chaudhury D, Walsh JJ, Friedman AK, Juarez B, Ku SM, Koo JW, et al. Rapid regulation of depression-related behaviours by control of midbrain dopamine neurons. Nature. 2013;493:532–6.

67. Dwivedi Y, Rizavi HS, Conley RR, Pandey GN. ERK MAP kinase signaling in post-mortem brain of suicide subjects: differential regulation of upstream Raf kinases Raf-1 and B-Raf. Mol Psychiatry. 2006;11:86–98.
68. Karege F, Perroud N, Burkhardt S, Fernandez R, Ballmann E, La Harpe R, et al. Protein levels of beta-catenin and activation state of glycogen synthase kinase-3beta in major depression. a study with postmortem prefrontal cortex. J Affect Disord. 2012;136:185–8.
69. Karege F, Perroud N, Burkhardt S, Schwald M, Ballmann E, La Harpe R, et al. Alteration in kinase activity but not in protein levels of protein kinase B and glycogen synthase kinase-3beta in ventral prefrontal cortex of depressed suicide victims. Biol Psychiatry. 2007;61:240–5.